Conservative Explicit Local Time-Stepping Schemes for The Rotating Shallow Water Equations

T.T. Phuong Hoang

Department of Mathematics and Statistics
Auburn University

SIAM GS19 - Mar 12, 2019
Houston, TX

Collaborators:

- Lili Ju, Zhu Wang (University of South Carolina)
- Wei Leng (LSEC, Chinese Academy of Sciences)
- Konstantin Pieper (Florida State University)

Acknowledgment:

- **US Department of Energy** as part of the project **E3SM** (**E**nergy **E**xascale **E**arth **S**ystem **M**odel), previously known as **ACME**, to develop the next generation of Earth System Models.

Reference:

- H., LENG, JU, WANG AND PIEPER, *Conservative explicit local time-stepping schemes for the shallow water equations*, J. Comput. Phys., 2019.

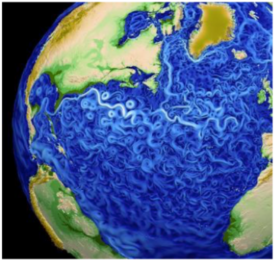

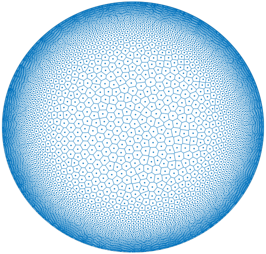

Figure courtesy of MPAS-Ocean.

[1] **MPAS**: **M**odel for **P**rediction **A**cross **S**cales
Project funded by the Department Of Energy (DOE)

Ocean Modeling by **MPAS-Ocean** [1]

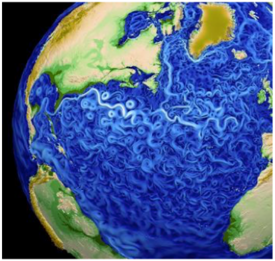 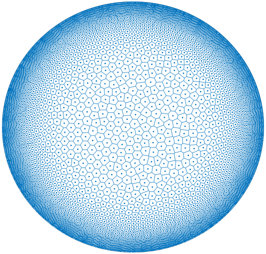

Figure courtesy of MPAS-Ocean.

- Large-scale, nonlinear problems $\longrightarrow$ **explicit** time-stepping & parallel simulation.

[1]**MPAS**: **M**odel for **P**rediction **A**cross **S**cales
Project funded by the Department Of Energy (DOE)

Ocean Modeling by **MPAS-Ocean** [1]

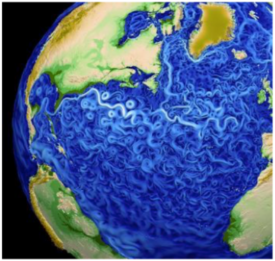
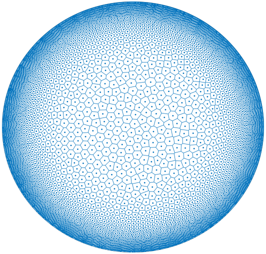

Figure courtesy of MPAS-Ocean.

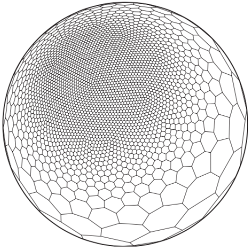

Multi-resolution Voronoi mesh
[Figure reprinted from Ringler et al. (2011)]

- Large-scale, nonlinear problems $\longrightarrow$ **explicit** time-stepping & parallel simulation.
- Multi-resolution meshes $\longrightarrow$ time step sizes restricted by **the size of the smallest cell**.

$\Longrightarrow$ Multi-scale time stepping algorithms.

[1] **MPAS**: **M**odel for **P**rediction **A**cross **S**cales
Project funded by the Department Of Energy (DOE)

Efficient local time-stepping (LTS) schemes for MPAS-Ocean

- Spatially-dependent time steps

  $\longrightarrow$ local CFL conditions for stability.

- Explicit schemes

  $\longrightarrow$ parallel, easy to incorporate into MPAS-Ocean.

- Conservation properties.

- Desired high-order accuracy in time.

Literature review

LTS algorithms of predictor-corrector type

- Osher and Sanders (1983): first order in space (finite volume discretization) and in time (explicit Euler)
- Dawson and Kirby (2001): second-order in space (high resolution methods with slope limiters) and in time (Heun's method)
- Sanders (2008): Godunov-type finite volume method, efficiency of a first-order LTS algorithm in term of computational cost via extensive numerical experiments.
- Krivodonova (2010): second-order in space (discontinuous Galerkin methods) and in time (Heun's method); Ashbourne (2016): extensions to third and fourth order Runge-Kutta methods.
- Trahan and Dawson (2012): Runge-Kutta discontinuous Galerkin finite elements, first-order accurate in time near the local time-stepping interface.

Literature review

LTS algorithms of predictor-corrector type

- Osher and Sanders (1983): first order in space (finite volume discretization) and in time (explicit Euler)
- Dawson and Kirby (2001): second-order in space (high resolution methods with slope limiters) and in time (Heun's method)
- Sanders (2008): Godunov-type finite volume method, efficiency of a first-order LTS algorithm in term of computational cost via extensive numerical experiments.
- Krivodonova (2010): second-order in space (discontinuous Galerkin methods) and in time (Heun's method); Ashbourne (2016): extensions to third and fourth order Runge-Kutta methods.
- Trahan and Dawson (2012): Runge-Kutta discontinuous Galerkin finite elements, first-order accurate in time near the local time-stepping interface.

Other approaches

- Berger and Oliger (84), Berger and LeVeque (98): adaptive mesh refinement methods
- Constantinescu and Sandu (07, 09): multi-rate time-stepping methods
- Grote, Mehlin and Mitkova (15): Runge-Kutta based LTS algorithms
- ...

The model equations

Nonlinear SWEs in vector-invariant form

$$\frac{\partial h}{\partial t} + \nabla \cdot (h\boldsymbol{u}) = 0, \tag{1}$$

$$\frac{\partial \boldsymbol{u}}{\partial t} + q(h\boldsymbol{u}^{\perp}) = -g\nabla(h+b) - \nabla K, \tag{2}$$

- h: fluid thickness, $\boldsymbol{u}$: fluid vector velocity,
- $\boldsymbol{k}$: unit vector pointing in the local vertical direction,
- $\boldsymbol{u}^{\perp} = \boldsymbol{k} \times \boldsymbol{u}$: the velocity rotated through a right angle,
- $q = \frac{\eta}{h}$: potential vorticity, $\eta = \boldsymbol{k} \cdot \nabla \times \boldsymbol{u} + f$: the absolute vorticity,
- $K = |\boldsymbol{u}|^2/2$: the kinetic energy,
- g: gravity, f: Coriolis parameter and b: bottom topography.

Multi-resolution Spherical Centroidal Voronoi Tessellations (SCVTs)

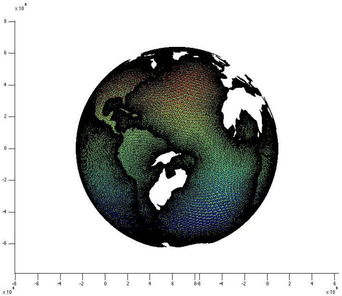

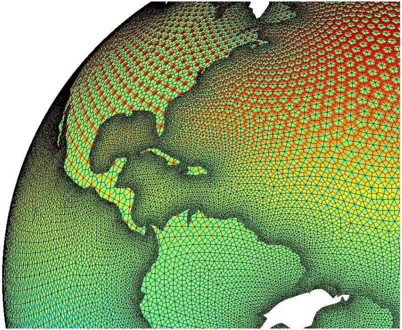

A multi-resolution Voronoi-Delaunay mesh by SCVT with 27,857 grid points

Spatial discretization: TRiSK[2] scheme

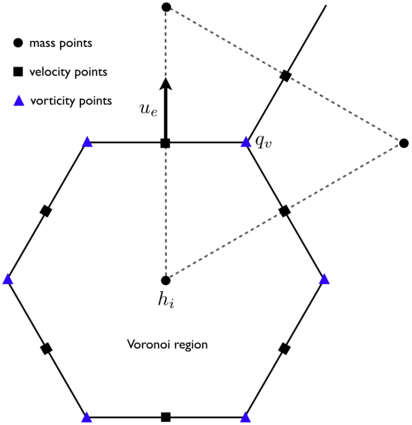

- **C-grid staggering**
  - Primal mesh: a Voronoi tessellation
  - Orthogonal dual mesh: its associated Delaunay triangulation
  - h_i: the mean thickness over primal cell P_i
  - u_e: the component of the velocity vector in the direction normal to primal edges
  - q_v: the mean vorticity (curl of the velocity) over dual cell D_v
- **Finite volume discretization**

[2] **TRiSK**: **T**hurburn, **Ri**ngler, **S**kamarock and **K**lemp (JCP, 2009).

Properties of TRiSK scheme

- Exact conservation of **mass**.
- Conservation of total energy (sum of the potential and kinetic energy) up to time truncation error.
- Robust simulation of potential vorticity.
  - ensuring the accuracy and physical correctness of the simulation of geophysical flows
- Good performance on highly variable spatial meshes.
- Accuracy in space: between first- and second-order.
  - depending on the quality of the meshes used

Explicit SSP-RK time-stepping

- System of ODEs resulting from spatial discretization:

$$\partial_t \boldsymbol{V} = F(\boldsymbol{V}).$$

- Strong Stability Preserving Runge-Kutta (SSP-RK) time-stepping:
  1. Forward Euler

$$\boldsymbol{V}_{n+1} = \boldsymbol{V}_n + \Delta t_n F(\boldsymbol{V}_n).$$

Explicit SSP-RK time-stepping

- System of ODEs resulting from spatial discretization:

$$\partial_t \boldsymbol{V} = F(\boldsymbol{V}).$$

- Strong Stability Preserving Runge-Kutta (SSP-RK) time-stepping:
  1. Forward Euler

$$\boldsymbol{V}_{n+1} = \boldsymbol{V}_n + \Delta t_n F(\boldsymbol{V}_n).$$

  2. SSP-RK2 (Heun's method)

$$\begin{aligned}
\overline{\boldsymbol{V}}_{n+1} &= \boldsymbol{V}_n + \Delta t_n F(\boldsymbol{V}_n), \\
\boldsymbol{V}_{n+1} &= \frac{1}{2}\boldsymbol{V}_n + \frac{1}{2}\left(\overline{\boldsymbol{V}}_{n+1} + \Delta t_n F(\overline{\boldsymbol{V}}_{n+1})\right).
\end{aligned}$$

Explicit SSP-RK time-stepping

- System of ODEs resulting from spatial discretization:

$$\partial_t \boldsymbol{V} = F(\boldsymbol{V}).$$

- Strong Stability Preserving Runge-Kutta (SSP-RK) time-stepping:
  1. Forward Euler

$$\boldsymbol{V}_{n+1} = \boldsymbol{V}_n + \Delta t_n F(\boldsymbol{V}_n).$$

  2. SSP-RK2 (Heun's method)

$$\begin{aligned}
\overline{\boldsymbol{V}}_{n+1} &= \boldsymbol{V}_n + \Delta t_n F(\boldsymbol{V}_n), \\
\boldsymbol{V}_{n+1} &= \frac{1}{2}\boldsymbol{V}_n + \frac{1}{2}\left(\overline{\boldsymbol{V}}_{n+1} + \Delta t_n F(\overline{\boldsymbol{V}}_{n+1})\right).
\end{aligned}$$

  3. SSP-RK3

$$\begin{aligned}
\overline{\boldsymbol{V}}_{n+1} &= \boldsymbol{V}_n + \Delta t_n F(\boldsymbol{V}_n), \\
\overline{\boldsymbol{V}}_{n+1/2} &= \frac{3}{4}V_n + \frac{1}{4}\left(\overline{\boldsymbol{V}}_{n+1} + \Delta t_n F(\overline{\boldsymbol{V}}_{n+1})\right), \\
\boldsymbol{V}_{n+1} &= \frac{1}{3}V_n + \frac{2}{3}\left(\overline{\boldsymbol{V}}_{n+1/2} + \Delta t_n F(\overline{\boldsymbol{V}}_{n+1/2})\right).
\end{aligned}$$

  4. Higher-order SSP-RK

Local time-stepping (LTS)

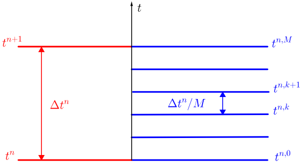

$$\left[t^n, t^{n+1}\right) = \bigcup_{k=0}^{M-1} \left[t^{n,k}, t^{n,k+1}\right)$$

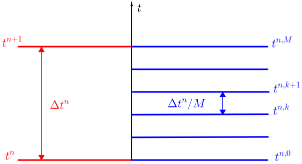

$$\left[t^n, t^{n+1}\right) = \bigcup_{k=0}^{M-1} \left[t^{n,k}, t^{n,k+1}\right)$$

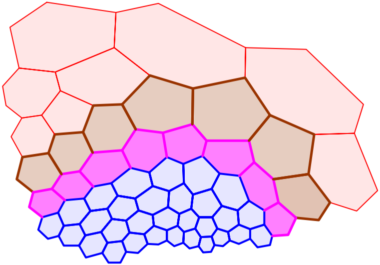

Cells/edges with fine time increments:

$\mathcal{F}_P$ & $\mathcal{F}_E$

Cells/edges with coarse time increments:

$\mathcal{C}_P^{\text{IF-L1}}$: interface-layer 1 cells

$\mathcal{C}_E^{\text{IF-L1}}$: interface-layer 1 edges

$\mathcal{C}_P^{\text{IF-L2}}$: interface-layer 2 cells

$\mathcal{C}_E^{\text{IF-L2}}$: interface-layer 2 edges

$\mathcal{C}_P^{\text{int}}$ & $\mathcal{C}_E^{\text{int}}$: internal 'coarse' cells & edges

Local time-stepping (LTS)

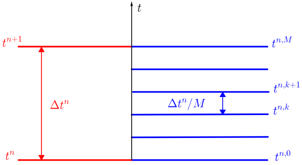

$$\left[t^n, t^{n+1}\right) = \bigcup_{k=0}^{M-1} \left[t^{n,k}, t^{n,k+1}\right)$$

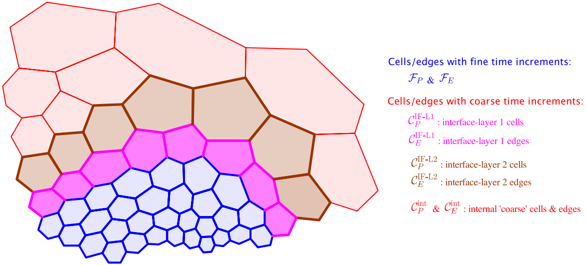

Conservative LTS algorithms:

- Predictor-corrector type
- Based on SSP-RK time-stepping and Taylor expansions

Second-order LTS predictor

The second-order predictor based on SSP-RK2 and Taylor expansion:

$$\begin{bmatrix} h_i^{n,k} \\ u_e^{n,k} \end{bmatrix} = (1-\alpha_k)\begin{bmatrix} h_i^{n} \\ u_e^{n} \end{bmatrix} + \alpha_k \begin{bmatrix} \overline{h}_i^{n+1} \\ \overline{u}_e^{n+1} \end{bmatrix},$$

$$\begin{bmatrix} \overline{h}_i^{n,k+1} \\ \overline{u}_e^{n,k+1} \end{bmatrix} = (1-\alpha_{k+1})\begin{bmatrix} h_i^{n} \\ u_e^{n} \end{bmatrix} + \alpha_{k+1} \begin{bmatrix} \overline{h}_i^{n+1} \\ \overline{u}_e^{n+1} \end{bmatrix},$$

for all $i \in \mathcal{C}_P^{\text{IF-L1}}$ and $e \in \mathcal{C}_E^{\text{IF-L1}}$, where

$$\alpha_k = \frac{k}{M}, \quad \text{for } k = 0, \ldots, M-1,$$

and $\overline{h}_i^{n+1}$ for $i \in \mathcal{C}_P^{\text{IF-L1}}$ and $\overline{u}_i^{n+1}$ for $e \in \mathcal{C}_E^{\text{IF-L1}}$ the values at the first stage of SSP-RK2 with a coarse time step.

$$\begin{bmatrix} h_i^{n,k} \\ u_e^{n,k} \end{bmatrix} = (1-\alpha_k-\widehat{\alpha}_k)\begin{bmatrix} h_i^{n} \\ u_e^{n} \end{bmatrix} + (\alpha_k-\widehat{\alpha}_k)\begin{bmatrix} \overline{h}_i^{n+1} \\ \overline{u}_e^{n+1} \end{bmatrix} + 2\widehat{\alpha}_k\begin{bmatrix} \overline{h}_i^{n+1/2} \\ \overline{u}_e^{n+1/2} \end{bmatrix},$$

$$\begin{bmatrix} \overline{h}_i^{n,k+1} \\ \overline{u}_e^{n,k+1} \end{bmatrix} = (1-\beta_k-\widehat{\beta}_k)\begin{bmatrix} h_i^{n} \\ u_e^{n} \end{bmatrix} + (\beta_k-\widehat{\beta}_k)\begin{bmatrix} \overline{h}_i^{n+1} \\ \overline{u}_e^{n+1} \end{bmatrix} + 2\widehat{\beta}_k\begin{bmatrix} \overline{h}_i^{n+1/2} \\ \overline{u}_e^{n+1/2} \end{bmatrix},$$

$$\begin{bmatrix} \overline{h}_i^{n,k+1/2} \\ \overline{u}_e^{n,k+1/2} \end{bmatrix} = (1-\gamma_k-\widehat{\gamma}_k)\begin{bmatrix} h_i^{n} \\ u_e^{n} \end{bmatrix} + (\gamma_k-\widehat{\gamma}_k)\begin{bmatrix} \overline{h}_i^{n+1} \\ \overline{u}_e^{n+1} \end{bmatrix} + 2\widehat{\gamma}_k\begin{bmatrix} \overline{h}_i^{n+1/2} \\ \overline{u}_e^{n+1/2} \end{bmatrix},$$

for all $i \in \mathcal{C}_P^{\text{IF-L1}}$ and $e \in \mathcal{C}_E^{\text{IF-L1}}$, where

$$\alpha_k = \frac{k}{M}, \quad \widehat{\alpha}_k = \frac{k^2}{M^2}, \quad \beta_k = \frac{k+1}{M}, \quad \widehat{\beta}_k = \frac{k(k+2)}{M^2}, \quad \gamma_k = \frac{2k+1}{2M}, \quad \widehat{\gamma}_k = \frac{2k^2+2k+1}{2M^2},$$

for $k = 0, \ldots, M-1$, $\overline{h}_i^{n+1}, \overline{h}_i^{n+1/2}$ for $i \in \mathcal{C}_P^{\text{IF-L1}}$ and $\overline{u}_i^{n+1}, \overline{u}_i$ for $e \in \mathcal{C}_E^{\text{IF-L1}}$ the values at the first two stages of SSP-RK3 with a coarse time step.

Properties of the LTS schemes

- A unified approach to construct high-order, explicit LTS schemes in which different time-step sizes are used in different regions of the domain, global CFL condition replaced by local CFL condition .

  $\longrightarrow$ time step sizes chosen according to local mesh sizes.

- By construction, all properties of the spatial discretization are preserved: exact conservation of the mass and potential vorticity, and conservation of the total energy within time-truncation errors.

- Implementation: in parallel and can be incorporated into MPAS-Ocean straightforwardly.

  $\Longrightarrow$ LTS is efficient in terms of stability, accuracy and computational cost.

Numerical results for the SWTC5 [3]

- On the sphere with a radius of $a = 6371.22\text{km}$.
- An isolated mountain is placed around the point with longitude and latitude

$$(\lambda_c, \theta_c) = (3\pi/2, \pi/6)$$

with height as $h_s = h_{s_0}(1 - r/R)$, where $h_{s_0} = 2\text{km}$, $R = \pi/9$, $r^2 = \min\{R^2, (\lambda - \lambda_c)^2 + (\theta - \theta_c)^2\}$, and (λ, θ) is the latitude and longitude.

- The initial longitudinal and latitudinal components of velocity are $(u, v) = (u_0 \cos(\theta), 0)$, where $u_0 = 20\text{ms}^{-1}$.
- The initial thickness is

$$h = h_0 - \frac{1}{g}(a\Omega u_0 + \frac{u_0^2}{2})(\sin(\theta))^2,$$

where $h_0 = 5.96\text{km}$, $\Omega = 7.292 \times 10^{-5}\text{s}^{-1}$, and $g = 9.80616\text{ms}^{-2}$.

[3] **Williamson et al.**, *A standard test set for numerical approximations to the shallow water equations in spherical geometry*, J. Comput. Phys., 1992.

The SWTC5 (Contd.)

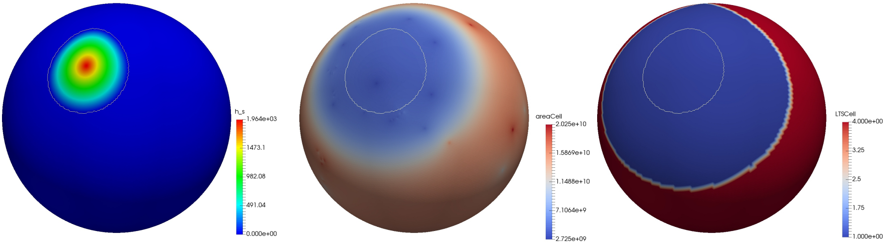

- Left: the bottom topography b
- Middle: the cell area of a variable-resolution SCVT mesh:
  - 40,962 cells
  - the coarse cell size is approximately two times of the fine cell size;
- Right: the LTS interface, $\Delta t_{\text{fine}} = \dfrac{\Delta t_{\text{coarse}}}{M}$

Accuracy in time: third-order LTS scheme

- 1 day simulation
- Fixed $M = 4$, varying Δt

Δt_{coarse}	h	[CR]	$\boldsymbol{u}$	[CR]
0.5α	3.38e-06	–	2.20e-05	–
0.25α	5.88e-07	[2.52]	3.27e-06	[2.75]
0.125α	7.80e-08	[2.91]	4.20e-07	[2.96]
0.0625α	1.24e-08	[2.85]	6.25e-08	[2.93]

- Fixed $\Delta t = 0.25\alpha$, varying M

M	h	$\boldsymbol{u}$
1	1.69e-06	9.38e-06
2	6.76e-07	3.68e-06
4	5.95e-07	3.27e-06
8	5.88e-07	3.25e-06

Evolution of fluid height for 15 days

(Loading ...)

Evolution of total energy

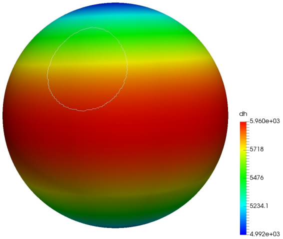

Initial fluid height $dh_0 = h_0 + b$

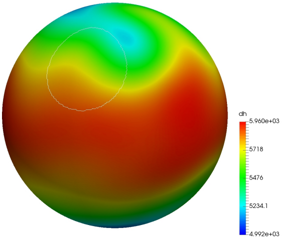

Fluid height at $T = 15$ days

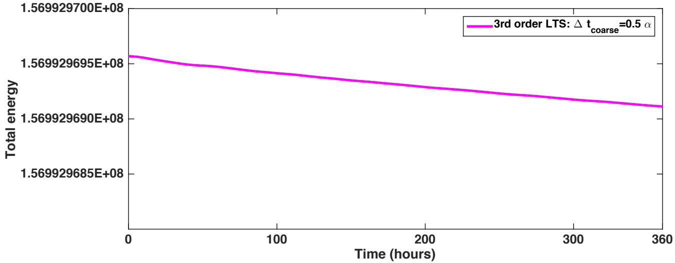

Exact conservation of mass and potential vorticity, $M = 4$

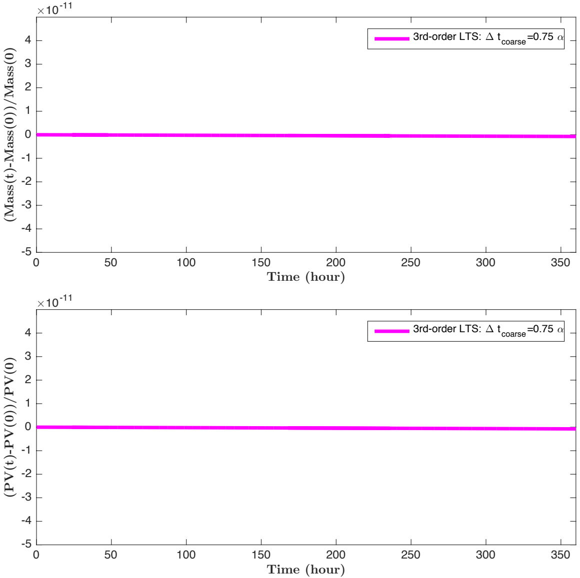

Parallel scalability: $\Delta t_{\text{coarse}} = 0.5\alpha$ and $M = 4$, $T = 3$ hours

No of Cores	**40,962** Cells			**163,842** Cells			**655,362** Cells		
	Time	Speedup	Efficiency	Time	Speedup	Efficiency	Time	Speedup	Efficency
The SSP-RK3 based LTS algorithm									
1	398.50	-	-	1704.73	-	-	7220.48	-	-
2	207.41	1.92	96.1%	838.29	2.03	101.7%	3543.05	2.04	101.9%
4	109.93	3.62	90.6%	420.18	4.06	101.4%	1745.22	4.14	103.4%
8	58.23	6.84	85.6%	213.74	7.98	99.7%	889.65	8.12	101.5%
16	31.82	12.52	78.3%	110.45	15.43	96.5%	461.69	15.64	97.7%
32	18.97	21.00	65.6%	57.51	29.64	92.6%	236.77	30.50	95.3%
64	10.86	36.70	57.4%	30.94	55.10	86.1%	115.57	62.47	97.6%
128	6.93	57.51	44.9%	17.18	99.20	77.5%	60.43	119.48	93.3%

Running times of Local time-stepping vs Global time-stepping

- Spatial mesh of 655,362 cells: fine region with 216,701 cells, and coarse region with 438,661 cells.
- Global SSP-RK3 time-stepping: uniform time step size $\Delta t = 0.125\alpha$.
- Local SSP-RK3 time-stepping: $\Delta t_{\text{coarse}} = 0.5\alpha$ and $\Delta t_{\text{fine}} = 0.125\alpha$ (i.e., $M = 4$).

No. of Cores	The SSP-RK3 algorithm		
	Without LTS	With LTS	Ratio
1	14476.94	7220.48	2.00
2	7021.38	3543.05	1.98
4	3348.39	1745.22	1.92
8	1722.99	889.65	1.94
16	883.58	461.69	1.91
32	463.39	236.77	1.96
64	229.58	115.37	1.99
128	119.57	60.43	1.98

Running times of Local time-stepping vs Global time-stepping

- Spatial mesh of 655,362 cells: fine region with 216,701 cells, and coarse region with 438,661 cells.
- Global SSP-RK3 time-stepping: uniform time step size $\Delta t = 0.125\alpha$.
- Local SSP-RK3 time-stepping: $\Delta t_{\text{coarse}} = 0.5\alpha$ and $\Delta t_{\text{fine}} = 0.125\alpha$ (i.e., $M = 4$).

No. of Cores	The SSP-RK3 algorithm		
	Without LTS	With LTS	Ratio
1	14476.94	7220.48	2.00
2	7021.38	3543.05	1.98
4	3348.39	1745.22	1.92
8	1722.99	889.65	1.94
16	883.58	461.69	1.91
32	463.39	236.77	1.96
64	229.58	115.37	1.99
128	119.57	60.43	1.98

- Theoretically optimal value for the ratio:

$$\frac{(4 \times 655362)}{(1 \times 438661 + 4 \times 216701)} \approx 2.01.$$

(when the cost for interface predictions and corrections is considered to be negligible).

Conclusions

Summary

- Conservative, explicit LTS algorithms in time for SWEs discretized in space by the TRiSK scheme.
- Time step sizes are restricted by local CFL conditions, instead of by the global CFL condition.
- Numerical results confirm the accuracy, stability and efficiency of LTS algorithms on variable spatial meshes.

Ongoing and future work

- High-order LTS algorithms for conservation laws.
- Numerical simulation of realistic benchmark test cases.
- Extensions of LTS to ocean/coastal coupling.